NEUROSCIENCE

Control of species-dependent cortico-motoneuronal connections underlying manual dexterity

Zirong Gu,[1] John Kalambogias,[2,3] Shin Yoshioka,[1] Wenqi Han,[4] Zhuo Li,[4,5] Yuka Imamura Kawasawa,[4,6] Sirisha Pochareddy,[4] Zhen Li,[4] Fuchen Liu,[4] Xuming Xu,[4] H. R. Sagara Wijeratne,[7] Masaki Ueno,[1,8] Emily Blatz,[1] Joseph Salomone,[1] Atsushi Kumanogoh,[9] Mladen-Roko Rasin,[7] Brian Gebelein,[1] Matthew T. Weirauch,[10] Nenad Sestan,[4] John H. Martin,[2,3]* Yutaka Yoshida[1]*

Superior manual dexterity in higher primates emerged together with the appearance of cortico-motoneuronal (CM) connections during the evolution of the mammalian corticospinal (CS) system. Previously thought to be specific to higher primates, we identified transient CM connections in early postnatal mice, which are eventually eliminated by Sema6D-PlexA1 signaling. *PlexA1* mutant mice maintain CM connections into adulthood and exhibit superior manual dexterity as compared with that of controls. Last, differing *PlexA1* expression in layer 5 of the motor cortex, which is strong in wild-type mice but weak in humans, may be explained by FEZF2-mediated cis-regulatory elements that are found only in higher primates. Thus, species-dependent regulation of *PlexA1* expression may have been crucial in the evolution of mammalian CS systems that improved fine motor control in higher primates.

The emergence of sophisticated motor and cognitive abilities in humans has been accompanied by complex central nervous system specializations. Axon trajectory and connectivity modifications contributed to an advanced brain that enabled higher cognitive functions and finer motor control (*1*). Species differences in axonal trajectories, circuit connectivity, and function are exemplified by the corticospinal (CS) tract (CST), which is essential for voluntary movement. A key feature distinguishing the CS systems of higher primates is hand dexterity control. This dexterity likely arises from the particular monosynaptic connections between CS neurons and motor neurons (MNs) that control hand muscles in higher primates (*2*). In other mammals, these cortico-motoneuronal (CM) connections may fail to develop, or they may form and then become actively eliminated. CS circuit pathways also differ substantially, with CSTs in higher primates descending within the ventral and lateral funiculi of the spinal cord, and those in rodents descending in the dorsal funiculus (*2*).

There are neither substantial contacts between CST axons and MNs nor functional CM connections in adult rodents (*3*–*6*). To examine early postnatal mice for CM connections, we performed monosynaptic rabies virus tracing from forelimb muscles at postnatal day 3 (P3) (Fig. 1A). When motor cortices were analyzed for mCherry expression 8 days after injection, we observed mCherry$^+$ CS neurons in both hemispheres with more extensive contralateral labeling (Fig. 1, B and D), providing evidence of CM connections in juvenile mice.

We then labeled CST fibers genetically using *Emx1-Cre;cc-GFP* mice and examined the postnatal CST innervation patterns within the spinal cord (fig. S1, A and C to M). In P2 mice, enhanced green fluorescent protein–labeled (eGFP$^+$) CST axons were detected in the ventral-most region of the dorsal funiculus (dCST) at upper cervical levels only (fig. S1, C to E). We also observed eGFP$^+$ CST fibers in the ventral and lateral funiculi (vCST and lCST; together, vlCST) at cervical, thoracic, and lumbar levels at P2 (fig. S1, C to K and N, purple bars). The density of the eGFP$^+$ vlCST decreased at P10 and was undetectable at P14 and later (fig. S1, B and L to N). Unilateral injections of *AAV1-hSyn-Cre* into the motor cortex of *ccGFP* mice at P4 led to vlCST labeling in the ipsilateral spinal cord at P10 (fig. S2, A to F). The vlCST constituted ~20% of all the descending CSTs (fig. S2, G to J). Analysis of the cervical spinal cords of P2 or P7 mice showed that presynaptic terminals of the ipsilateral vlCST or contralateral dCST form contacts on MNs (fig. S2, K and L).

Next, we examined whether the semaphorin (Sema) family of repulsive (or attractive) molecules and their receptors [plexins (Plexs) and neuropilins (Npns)] are involved in axon pruning of the vlCST and the elimination of CM connections (fig. S3, A to E). Targeted deletions of those receptors revealed that only *PlexA1$^{fl/fl}$;Emx1-Cre* mice retained CST axons in the ventral and lateral funiculi until P38 (Fig. 1, E to P). Both Sema6C and Sema6D are PlexA1 ligands; however, only mice lacking Sema6D exhibited persistent vlCSTs (Fig. 1, M to P, and fig. S3, L and M). No obvious defects were found in CST trajectories around the decussation region of *PlexA1* and *Sema6D* mutant mice (fig. S4).

The PlexA1 receptor and *Sema6D* were expressed in CS axons in the brain (fig. S5) and in the ventral spinal cord and white matter, respectively, with *Sema6D* expression relatively restricted to P6 mice (fig. S6, E to J). CS circuit labeling by use of dual-color retrograde virus tracing demonstrated that the dCST and vlCST in adult *PlexA1$^{fl/fl}$;Emx1-Cre* mice were derived from the same CS neurons (fig. S7).

Anterograde tracing in adult mice revealed more numerous contacts between the CST and MNs in *PlexA1$^{fl/fl}$;Emx1-Cre* mice as compared with controls (fig. S8) without any obvious defects in projection patterns to brainstem motor pathways (fig. S9), which is consistent with *Sema6D* expression being restricted to the spinal cord and absent from those brain regions (fig. S6, A to D). A dorsal hemisection lesion at the C3/4 spinal level in adult mice followed by removal of the dCST below the lesion site (fig. S10A) revealed that individual vlCST axons produced multiple collaterals, some of which crossed the midline, exhibiting arborization patterns that were similar to those described in adult rhesus monkey CSTs (fig. S10) (*7*, *8*). Monosynaptic rabies virus assays revealed a significant increase in CM connections in early postnatal *PlexA1* mutant mice compared with same-age controls (Fig. 1, A to D), with no changes in monosynaptic connections between MNs and premotor interneurons or other descending brainstem nuclei (figs. S11 to S13).

Because monosynaptic rabies virus tracing from muscles is ineffective after P10 (*9*), we performed electrophysiology to determine whether functional CM connections are maintained in adult *PlexA1$^{fl/fl}$;Emx1-Cre* mice. We used stimulus-triggered averaging (StTA) to detect the latency of post-stimulus facilitation (PStF) of electromyography (EMG) recorded from forelimb muscles in response to motor cortex stimulation (*10*). *PlexA1$^{fl/fl}$;Emx1-Cre* mice displayed shorter PStF latencies for both contralateral and ipsilateral CS circuits (Fig. 2, A to G, and fig. S14), with no obvious changes in the currents required to evoke PStF or the thresholds for conventional intracortical microstimulation (ICMS)

[1]Division of Developmental Biology, Cincinnati Children's Hospital Medical Center (CCHMC), Cincinnati, OH 45229, USA. [2]Department of Cellular, Molecular, and Biomedical Sciences, City University of New York School of Medicine, New York, NY 10031, USA. [3]Graduate Center, City University of New York, New York, NY 10017, USA. [4]Department of Neuroscience, Kavli Institute for Neuroscience, Yale School of Medicine, New Haven, CT 06510, USA. [5]Basic Medical School of Zhengzhou University, Zhengzhou, Henan, 450001, P.R. China. [6]Institute for Personalized Medicine, Departments of Biochemistry and Molecular Biology and Pharmacology, Penn State College of Medicine, PA 17033, USA. [7]Department of Neuroscience and Cell Biology, Robert Wood Johnson Medical School, Rutgers University, Piscataway, NJ 08854, USA. [8]Precursory Research for Embryonic Science and Technology (PRESTO), Japan Science and Technology Agency (JST), Kawaguchi, Saitama, 332-0012, Japan. [9]Department of Respiratory Medicine and Clinical Immunology, Graduate School of Medicine, Osaka University, Suita, 565-0871, Japan. [10]Center for Autoimmune Genomics and Etiology, Division of Biomedical Informatics, and Division of Developmental Biology, Cincinnati Children's Hospital Medical Center, Cincinnati, OH 45229, USA.
*Corresponding author. Email: yutaka.yoshida@cchmc.org (Y.Y.); jmartin@ccny.cuny.edu (J.H.M.)

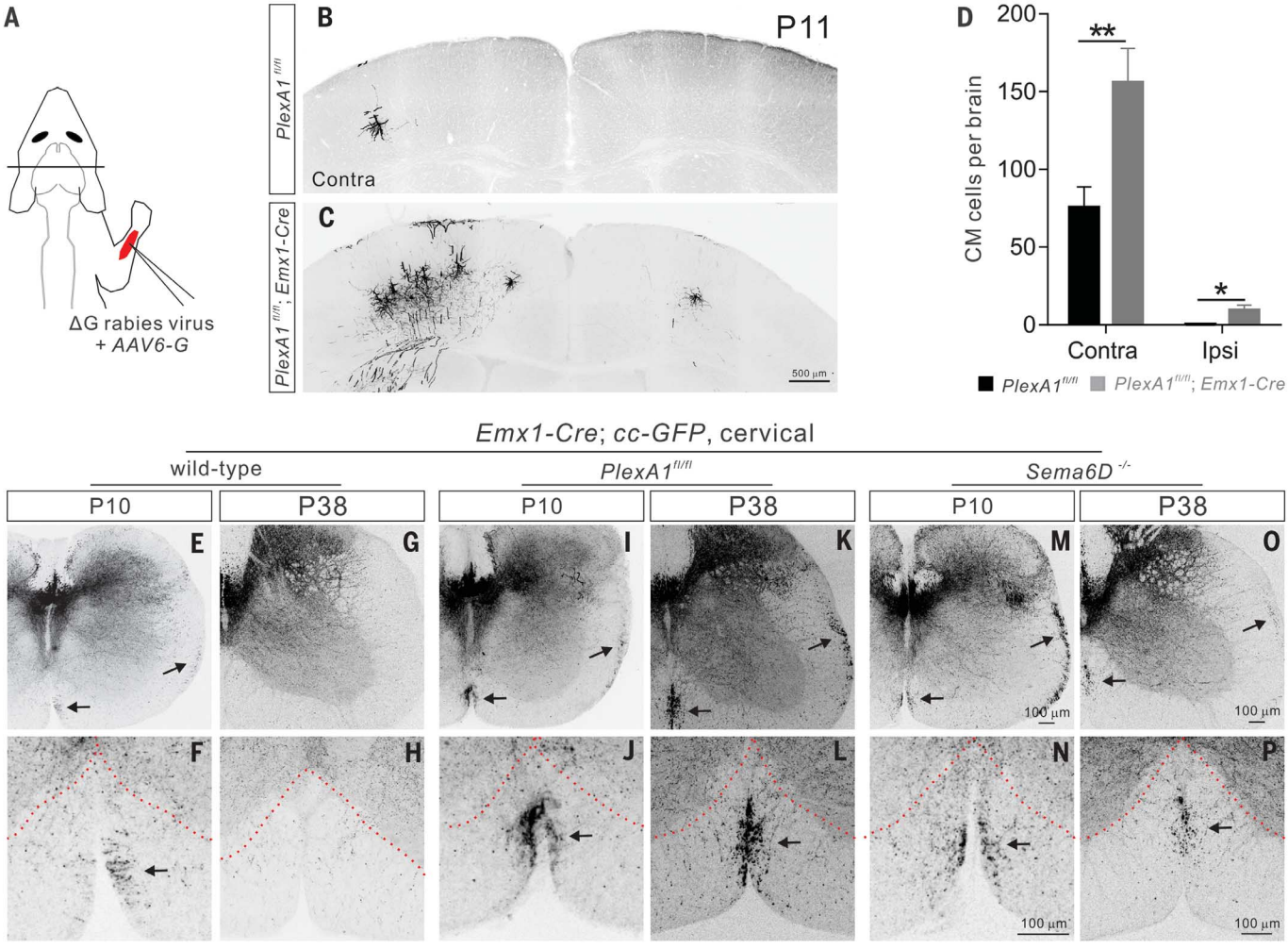

Fig. 1. Elimination of CM connections and the vlCST by Sema6D-PlexA1 signaling in early postnatal mice. (**A**) Experimental scheme for identifying CM connections. Rab-mCherry and *AAV6-G* were co-injected into forelimb muscles of P3 mice. (**B** and **C**) Coronal brain sections from (B) P11 control (*PlexA1*$^{fl/fl}$, *n* = 7) and (C) *PlexA1* mutant (*PlexA1*$^{fl/fl}$; *Emx1-Cre*, *n* = 8) mice showing labeling of CM cells 8 days after Rab-mCherry virus injections into forelimb muscles. Scale bar, 500 μm. (**D**) Quantification of CM cells. *$P < 0.05$, **$P < 0.01$. (**E** to **P**) Cervical spinal cord sections from wild-type [P10, (E) and (F); P38, (G) and (H)], *PlexA1*$^{fl/fl}$ [P10, (I) and (J); P38, (K) and (L)], and *Sema6D*$^{-/-}$ [P10, (M) and (N); P38, (O) and (P)] mice. Scale bars, 100 μm.

(fig. S15, A and B). We compared the PStF latencies from forelimb muscles after CST axon stimulation in the ventral portion of the C5 dorsal column (DC) (Fig. 2H). Antidromic field recordings from the motor cortex confirmed CST activation in our stimulation paradigm from this ventral stimulation site, but not from the dorsal portion of the DC, where ascending sensory fibers reside (Fig. 2, I and J, and fig. S16). PStF latencies evoked through ventral DC stimulation (CST) in *PlexA1*$^{fl/fl}$*;Emx1-Cre* mice were significantly shorter than those observed in *PlexA1*$^{fl/fl}$ mice (Fig. 2, K to N), whereas stimulation of the dorsal DC showed no differences in evoked EMG responses between control and *PlexA1*$^{fl/fl}$*;Emx1-Cre* mice (fig. S17). Furthermore, we found that current amplitudes used to evoke EMG responses through either the dorsal DC (afferent fibers) or the ventral DC (CST) were similar between control and *PlexA1*$^{fl/fl}$*;Emx1-Cre* mice (fig. S15, C and D).

CM connections are critical for fine manual dexterity in primates (*11*, *12*). Rodents show a limited degree of manual dexterity without CM connections by using coordinated paw movements to manipulate food pieces (*13*). To measure manual dexterity, we performed the capellini handling test (Fig. 3A and fig. S18, E to G) with mice that had received *AAV1-Cre* bilateral motor cortex injections at P2 (*PlexA1*$^{fl/fl}$*;AAV1-Cre* mice), which produces similar developmental pruning defects as those observed in the *Emx1-Cre*–mediated mutants (fig. S18, A to D). *PlexA1*$^{fl/fl}$*;AAV1-Cre* mice ate the capellini significantly faster than *PlexA1*$^{fl/+}$*;AAV1-Cre* mice on all testing days (Fig. 3B, fig. S18H, and movies S1 to S4) and exhibited significantly higher paw adjustment rates on all four testing days as compared with *PlexA1*$^{fl/+}$*;AAV1-Cre* mice (Fig. 3C and fig. S18I). In addition, *PlexA1*$^{fl/fl}$*;AAV1-Cre* mice displayed fewer atypical handling patterns than did *PlexA1*$^{fl/+}$*;AAV1-Cre* mice (Fig. 3D and fig. S18, J to Q). *PlexA1*$^{fl/fl}$*;Emx1-Cre* mice also outperformed control mice during a sticky tape removal test (fig. S19, A and B).

To evaluate grasping, we designed and implemented a new prehension test (fig. S20) in which animals had to use their paws to reach, grasp, and retrieve a food pellet (Fig. 3, E to G). *PlexA1*$^{fl/fl}$*;AAV1-Cre* mice exhibited significantly higher grasping success rates than those of controls (*PlexA1*$^{fl/+}$*;AAV1-Cre* and *PlexA1*$^{fl/fl}$*;AAV1-td*), whereas pellet consumption time was indistinguishable between the two groups (Fig. 3, H to K, and movies S5 and S6). We also found no obvious deficits in grip strength (fig. S19C) or grid-walking in *PlexA1*$^{fl/fl}$*;Emx1-Cre* mice (fig. S19D).

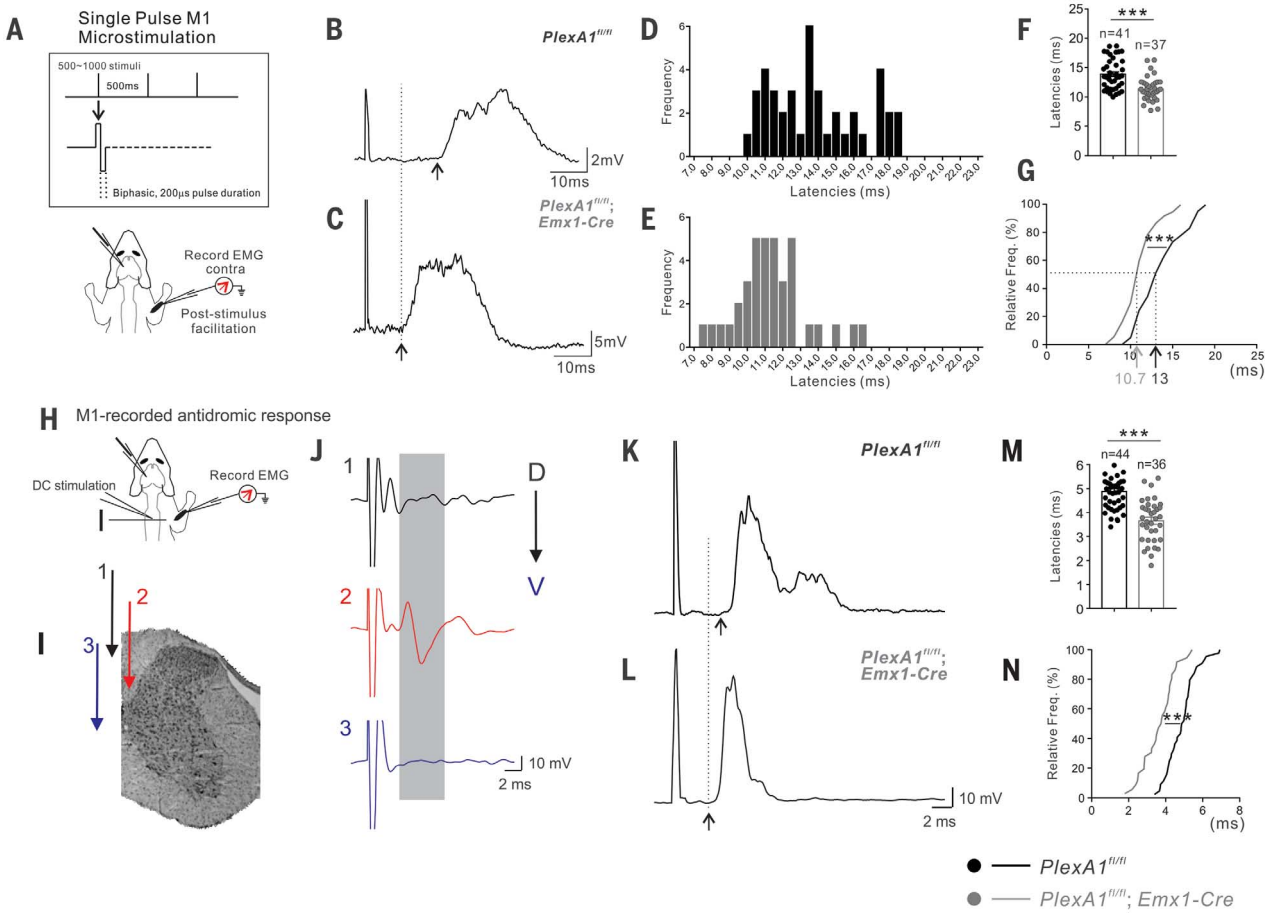

Fig. 2. Functional CM connections in adult *PlexA1*$^{fl/fl}$*;Emx1-Cre* mice. (**A**) Schematic diagram of experiment to examine PStF in adult mice (3 months or older). EMG recordings from contralateral flexor carpi radialis and biceps brachii muscles. (**B** and **C**) Contralateral PStF from (B) control (*PlexA1*$^{fl/fl}$) and (C) mutant (*PlexA1*$^{fl/fl}$*;Emx1-Cre*) mice. Dotted line indicates the onset of the EMG response in the mutant; arrows indicate EMG onsets. (**D** and **E**) Frequency distributions of contralateral PStF values from (D) control (*PlexA1*$^{fl/fl}$, $n = 6$; wild-type, $n = 3$) and (E) *PlexA1*$^{fl/fl}$*;Emx1-Cre* ($n = 8$) mice. (**F**) PStF latencies after motor cortex stimulation in *PlexA1*$^{fl/fl}$ (41 stimulation sites; median delay = 11.34 ms) and *PlexA1*$^{fl/fl}$*;Emx1-Cre* (37 stimulation sites; median delay = 13.88 ms) mice. ***$P < 0.001$. (**G**) Cumulative frequency distribution histogram. gray line, *PlexA1*$^{fl/fl}$*;Emx1-Cre* mice; black line, *PlexA1*$^{fl/fl}$ mice. ***$P < 0.001$. (**H**) Schematic diagram of DC electrical stimulation-evoked muscle PStF. (**I**) Section from a DC stimulation experiment, showing the three electrode locations used to evoke M1 antidromic responses. (**J**) Electrical stimulation of the ventral DC evokes an antidromic field potential in the motor cortex. 1, Dorsal DC stimulation, where afferent fibers are located; 2, ventral DC stimulation (where CST fibers are located); and 3, stimulation at the level of the central canal (**K** and **L**) PStF traces derived from average EMG responses evoked by ventral DC sites in (K) *PlexA1*$^{fl/fl}$ and (L) *PlexA1*$^{fl/fl}$; *Emx1-Cre* mice. Dotted line indicates the onset of the EMG response in the mutant; arrows indicate EMG onsets. (**M**) PStF latencies in *PlexA1*$^{fl/fl}$ (44 sites from 8 animals; median delay = 4.88 ms) and *PlexA1*$^{fl/fl}$*;Emx1-Cre* (36 sites from 6 animals; median delay = 3.66 ms) mice. ***$P < 0.001$. (**N**) Cumulative frequency distribution plot of PStF latencies from *PlexA1*$^{fl/fl}$*;Emx1-Cre* (gray line) and *PlexA1*$^{fl/fl}$ mice (black line). Arrows indicate the onsets of EMG responses [(B), (C), (K), and (L)]. ***$P < 0.001$.

Behavioral changes were not associated with any obvious changes in cortico-cortical projections, cortical lamination or dendritic development (by means of Golgi analysis) of CS neurons in *PlexA1*$^{fl/fl}$*;Emx1-Cre* mice (fig. S21).

The presence of CM connections and the vlCST in adult *PlexA1* mutant mice bear a remarkable resemblance to human CS circuits, prompting us to examine *PLEXA1* expression within the developing human motor cortex. Human midfetal cortices at 20 post-conceptional weeks (pcw), which corresponds to the early postnatal mouse cortex, showed very weak *PLEXA1* expression in layer 5 CS neurons, but strong expression in layer 6 of the putative motor cortex, which does not give rise to CST projections (Fig. 4A).

To determine whether species-dependent cis-regulatory elements might define *PLEXA1* expression levels in layer 5, we first identified and compared putative orthologous enhancer regions between humans and mice. Enhancers were identified on the basis of features indicative of active regulatory regions, including H3K4me3 and H3K27ac histone marks, deoxyribonuclease hypersensitivity, and DNA conservation across mammals. This resulted in a ~5-kb putative orthologous enhancer in humans and mice (fig. S22). Within the putative human enhancer, we identified a total of 28 putative FEZF2 binding sites. FEZF2 (also known as FEZL and ZFP312), encoding a zinc-finger transcription factor (*14*) required for CS tract development (*15*), was expressed in the putative layer 5 of the human late mid-fetal neocortex (fig. S26A) or in the putative layer 5 of the human brain at 22 pcw (fig. S26A). Three FEZF2 binding sites correspond to the typical "CTNCANCN" Fezf2 binding site (figs. S23 to S25, blue bars) (*16*), with the remaining 25 resembling a recently described "CGCCGC" element (figs. S23 to S25, green and red bars) (*17*). Five of the total 28 sites were conserved in both humans and mice (fig. S24, green bars), whereas 23 of them were only found in humans, resulting in a putative homotypic cluster

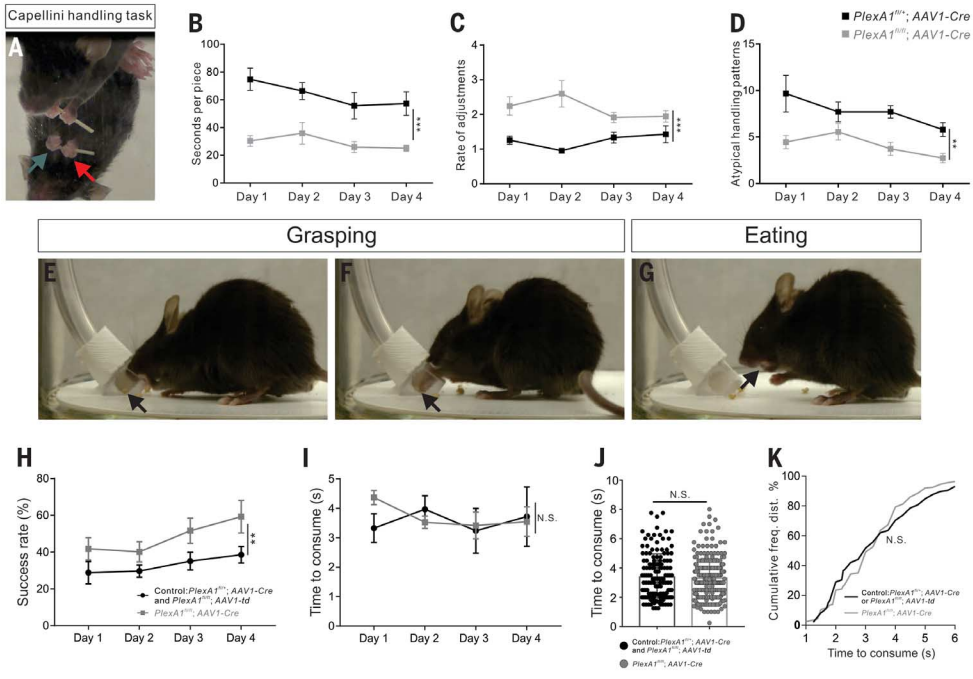

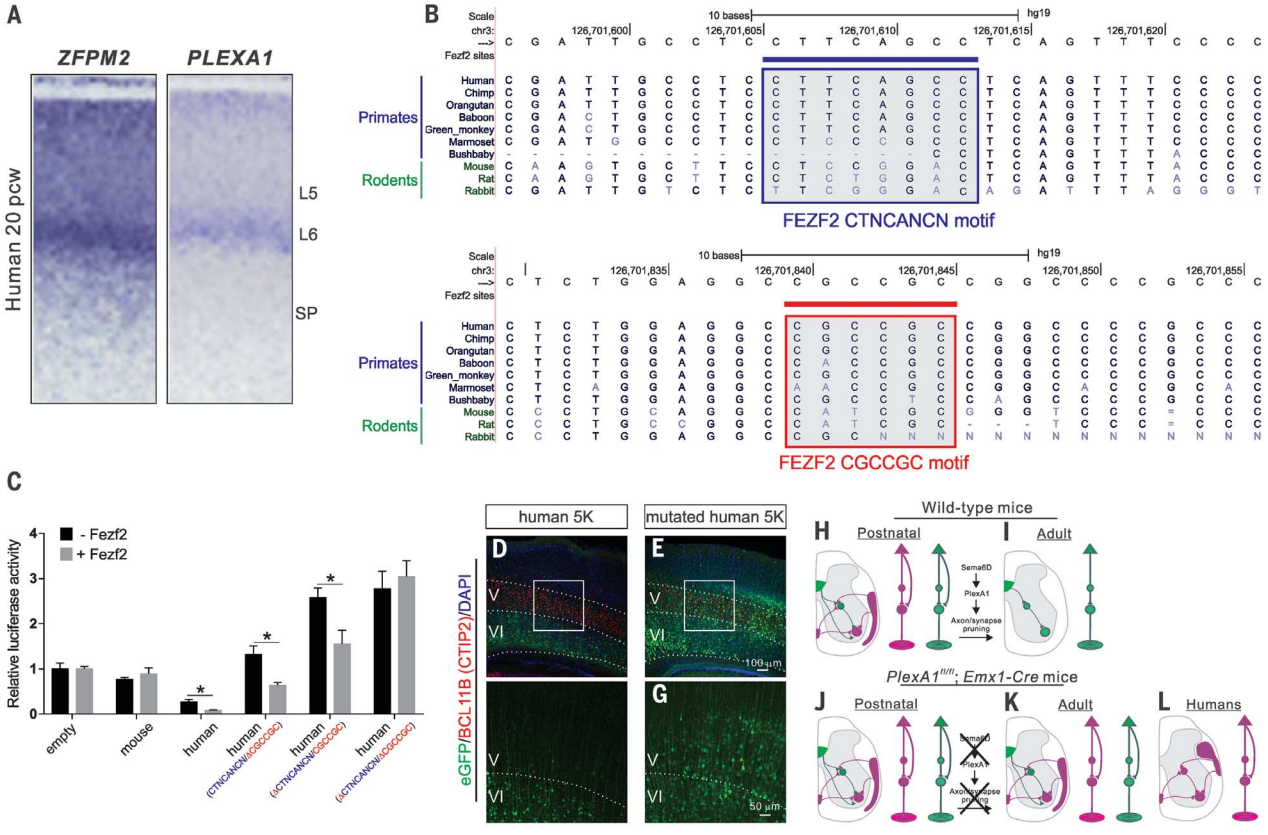

Fig. 3. Adult *PlexA1* mutant mice outperform controls in dexterous manipulation tasks. (**A**) Mouse performing the capellini handling test. Guiding and grasping hands are indicated by green and red arrows, respectively. (**B** to **D**) Results of the capellini handling test in 2-month-old control (*PlexA1*$^{fl/+}$;*AAV1-Cre*, *n* = 10) and *PlexA1*$^{fl/fl}$; *AAV1-Cre* (*n* = 10) mice during 4 testing days. Rate of adjustment is the average number of paw adjustments per piece/eating time. ***P* < 0.01, ****P* < 0.001. (**E** to **G**) A mouse during the grasping test. Food pellets are indicated by black arrows. (**H** and **I**) Grasping success and consumption time in 3-month-old control (*PlexA1*$^{fl/+}$;*AAV1-Cre*, *n* = 3; and *PlexA1*$^{fl/fl}$; *AAV1-td*, *n* = 4) and *PlexA1*$^{fl/fl}$;*AAV1-Cre* (*n* = 8) mice over 4 testing days. ***P* < 0.01. (**J** and **K**) Quantification and frequency distributions of pellet consumption time by control (145 trials) and *PlexA1*$^{fl/fl}$;*AAV1-Cre* (251 trials) mice.

Fig. 4. Expression of *PLEXA1* in layer 5 of the motor cortex in mice and humans, and FEZF2-mediated repression. (**A**) *ZFPM2* (*FOG2*) (layer 6 marker) (*15*) and *PLEXA1* in the human motor cortex at 20 pcw assessed by means of in situ hybridization. (**B**) Sequence conservation of putative *PlexA1* cis-regulatory elements. Multispecies DNA sequence alignment showing examples of FEZF2 CTNCANCN binding sites (top, blue bar and box) and CGCCGC binding sites (bottom, red bar and box). The motifs are highlighted by gray-filled boxes. (**C**) Luciferase activity of reporter constructs in a 293T cell line (expressing endogenous human *Fezf2*) with or without cotransfection with a human *FEZF2*-expressing vector. Error bars represent the SEM of triplicate experiments. **P* < 0.05. (**D** to **G**) Analysis of transgenic mice using a 5-kb region upstream from the first exon of the human *PLEXA1* gene or mutated human FEZF2 binding sequences. (**E** and **G**) High magnification view of the boxed areas in (D) and (F), respectively. (**H** to **L**) Summary of the axonal trajectories and CS connectivity within the cervical spinal cord in wild-type and *PlexA1*$^{fl/fl}$;*Emx1-Cre* mice, and in humans.

of 23 human FEZF2 binding sites (Fig. 4B and figs. S22A and S23 to S25) (*18*, *19*). Humans, chimpanzees, gorillas, orangutans, and baboons, which all have CM connections (*2*), all possess these FEZF2 binding sites in their putative *PlexA1* cis-regulatory elements (Fig. 4B and figs. S23 to S25). In contrast, mice, rats, and rabbits—as well as some primates that lack CM connections, such as marmosets and bushbabies (*2*)—either lack these FEZF2 binding sites completely or have nucleotide mismatches that are predicted to decrease FEZF2 binding (Fig. 4B and figs. S23 to S25). Electrophoretic mobility shift assays (EMSAs) demonstrated binding of FEZF2 to the human FEZF2 binding site but weaker binding to the homologous mouse sequence and human sequence with point mutations (making it identical to the mouse sequence) (fig. S26B).

Using in vitro luciferase assays, we found that FEZF2 represses the transcriptional activity of the human, but not mouse, cis-regulatory elements (Fig. 4C and fig. S26, C and D). Constructs with point mutations in both FEZF2 motifs showed a complete loss of FEZF2-mediated repression (Fig. 4C). Enhancer analysis by transfecting constructs with the FEZF2 cis-regulatory elements to primary cortical neuron cultures from wild-type and *Fezf2* mutant mice demonstrated a strong FEZF2-mediated repression of the putative human cis-regulatory elements in BCL11B$^+$ (CTIP2$^+$) layer 5 cortical neurons (figs. S27 and S28). Further analysis of transgenic mice expressing GFP under the human FEZF2 cis-regulatory elements revealed that the putative human cis-regulatory elements drove strong expression of GFP in layer 6, but not layer 5, of the motor cortex, recapitulating the *PLEXA1* expression in the human motor cortex (Fig. 4, D and E, and fig. S29). Transgenic mice with the human FEZF2 binding sites mutated drove robust expression in layer 5 neurons and CS axons (Fig. 4, F and G, and fig. S29). Expression of *PlexA1* was not altered in the cortices of *Fezf2* mutant mice at P0 (fig. S26, E and F).

Considering that CM connections seem beneficial for mice, why are they eliminated? Perhaps increased manual dexterity confers no fitness advantages to quadrupedal animals, or perhaps it even imposes a fitness burden. For example, maintenance of CM connections in mice may disrupt the development and function of other spinal motor circuits, such as those for forelimb locomotion rather than manipulation. Another question lies in the preservation of transient CM connections in wild-type mice. Perhaps they play a temporary developmental role in assisting the establishment of other spinal neural circuits. Our findings, providing insight into the specific contributions of CM connections to dexterous manipulations by mice, serve as a stepping stone toward answering these questions and present a potential mechanism for how CM connections emerged during mammalian evolution.

REFERENCES AND NOTES

1. L. Krubitzer, *Neuron* **56**, 201–208 (2007).
2. R. N. Lemon, *Annu. Rev. Neurosci.* **31**, 195–218 (2008).
3. H. W. Yang, R. N. Lemon, *Exp. Brain Res.* **149**, 458–469 (2003).
4. B. Alstermark, J. Ogawa, *J. Neurophysiol.* **92**, 1958–1962 (2004).
5. B. Alstermark, J. Ogawa, T. Isa, *J. Neurophysiol.* **91**, 1832–1839 (2004).
6. Y. Q. Jiang, B. Zaaimi, J. H. Martin, *J. Neurosci.* **36**, 193–203 (2016).
7. E. S. Rosenzweig, G. Courtine, D. L. Jindrich, J. H. Brock, A. R. Ferguson, S. C. Strand, Y. S. Nout, R. R. Roy, D. M. Miller, M. S. Beattie, L. A. Havton, J. C. Bresnahan, V. R. Edgerton, M. H. Tuszynski, *Nat. Neurosci.* **13**, 1505–1510 (2010).
8. M. C. Park, A. Belhaj-Saïf, P. D. Cheney, *J. Neurophysiol.* **92**, 2968–2984 (2004).
9. A. E. Stepien, M. Tripodi, S. Arber, *Neuron* **68**, 456–472 (2010).
10. E. E. Fetz, P. D. Cheney, D. C. German, *Brain Res.* **114**, 505–510 (1976).
11. R. Heffner, B. Masterton, *Brain Behav. Evol.* **12**, 161–200 (1975).
12. D. G. Lawrence, D. A. Hopkins, *Brain* **99**, 235–254 (1976).
13. R. P. Allred, D. L. Adkins, M. T. Woodlee, L. C. Husbands, M. A. Maldonado, J. R. Kane, T. Schallert, T. A. Jones, *J. Neurosci. Methods* **170**, 229–244 (2008).
14. T. Shimizu, M. Nakazawa, S. Kani, Y. K. Bae, T. Shimizu, R. Kageyama, M. Hibi, *Development* **137**, 1875–1885 (2010).
15. M. Shibata, F. O. Gulden, N. Sestan, *Trends Genet.* **31**, 77–87 (2015).
16. L. Chen, J. Zheng, N. Yang, H. Li, S. Guo, *J. Biol. Chem.* **286**, 18641–18649 (2011).
17. S. Lodato, B. J. Molyneaux, E. Zuccaro, L. A. Goff, H.-H. Chen, W. Yuan, A. Meleski, E. Takahashi, S. Mahony, J. L. Rinn, D. K. Gifford, P. Arlotta, *Nat. Neurosci.* **17**, 1046–1054 (2014).
18. V. Gotea, A. Visel, J. M. Westlund, M. A. Nobrega, L. A. Pennacchio, I. Ovcharenko, *Genome Res.* **20**, 565–577 (2010).
19. D. Ezer, N. R. Zabet, B. Adryan, *Comput. Struct. Biotechnol. J.* **10**, 63–69 (2014).

ACKNOWLEDGMENTS

We are grateful to M. Baccei, J. N. Betley, K. Campbell, S. Crone, C. Gu, T. Isa, D. Ladle, M. Nakafuku, and R. Yu for critical comments on the manuscript. We thank Boston Children's Hospital Viral Core (supported by core grant NEI 5P30EY012196-17) for making the AAV6-G virus. We thank P. Arlotta for the Fezf2 construct. Z.G. and E.B. were supported by the Graduate Summer Undergraduate Mentoring Program at the University of Cincinnati. M.T.W. is supported by the National Institutes of Health (NIH) grants R01 NS099068 and R21 HG008186, Lupus Research Alliance "Novel Approaches" award, and a CCHMC CpG Pilot Study award. N.S. is supported by NIH grants MH106934 and MH103339. J.H.M. and Y.Y. are supported by NIH grants NS079569 and NS093002, respectively. All data are available in the main texts and supplementary materials. Z.G. and Y.Y. conceived of the project and contributed to experimental design and interpretation. Z.G. performed most of the experiments. Z.G., J.K., and J.H.M. designed the cortico-muscular electrophysiology assay, performed EMG recordings, and analyzed and interpreted the electrophysiological data. Y.I.K., W.H., Z.L., Z.L., F.L., S.P., X.X., and N.S. performed the in situ hybridizations using human tissues, chromatin immunoprecipitation–sequencing using human and mouse tissues, and culture experiments using *Fezf2-floxed* mice. S.Y. contributed to cloning of the human and mouse genomic regions and the luciferase assays. E.B. performed the grid-walking test and contributed to the immunochemistry studies. M.U. purified rabies viruses and assisted in the dorsal hemisection surgery. H.R.S.W. and M.-R.R. analyzed the cortical layers and cortico-cortical projections and also conducted the Golgi analyses. J.S. and B.G. performed the EMSA analyses. M.T.W. performed the cross-species cis-regulatory element comparisons. A.K. provided the *Sema6D* mutant mice. Y.Y. supervised all aspects of the work, and Z.G., J.H.M, and Y.Y. prepared the manuscript with contributions from other authors.

SUPPLEMENTARY MATERIALS

www.sciencemag.org/content/357/6349/400/suppl/DC1
Materials and Methods
Figs. S1 to S29
References (*20*–*44*)
Movies S1 to S6

4 April 2017; accepted 12 June 2017
10.1126/science.aan3721

Control of species-dependent cortico-motoneuronal connections underlying manual dexterity

Zirong Gu, John Kalambogias, Shin Yoshioka, Wenqi Han, Zhuo Li, Yuka Imamura Kawasawa, Sirisha Pochareddy, Zhen Li, Fuchen Liu, Xuming Xu, H. R. Sagara Wijeratne, Masaki Ueno, Emily Blatz, Joseph Salomone, Atsushi Kumanogoh, Mladen-Roko Rasin, Brian Gebelein, Matthew T. Weirauch, Nenad Sestan, John H. Martin and Yutaka Yoshida

Science **357** (6349), 400-404.
DOI: 10.1126/science.aan3721

The disappearance of fine motor control

Manual skills are much better developed in primates than in rodents. This difference is in part due to species-specific differences in the control of motoneurons by the brain. Gu *et al.* used a range of approaches to evaluate potential corticospinal tract projections in neonatal mice. These projections exist immediately after birth but disappear within the first 2 postnatal weeks owing to the actions of plexin A, a member of the semaphorin receptor family. Targeted deletion of semaphorin receptors in mutant mice prevented elimination of corticospinal tract projection and loss of functional monosynaptic input to spinal motoneurons.

Science, this issue p. 400